Fan texture of the compound Ba3Co2Fe244O41 pre-aligned in a magnetic field

Document status and date:
Published: 01/01/1970

Document Version:
Publisher's PDF, also known as Version of Record (includes final page, issue and volume numbers)

Please check the document version of this publication:

• A submitted manuscript is the version of the article upon submission and before peer-review. There can be important differences between the submitted version and the official published version of record. People interested in the research are advised to contact the author for the final version of the publication, or visit the DOI to the publisher's website.
• The final author version and the galley proof are versions of the publication after peer review.
• The final published version features the final layout of the paper including the volume, issue and page numbers.
[Link to publication](#)

Fan Texture of the Compound Ba₃Co₂Fe₂₄O₄₁ Pre-aligned in a Magnetic Field

BY E. M. C. HUIJSER-GERITS, G. D. RIECK AND D. L. VOGEL

Laboratory of Physical Chemistry, Technological University, Eindhoven, The Netherlands

Samples of the ferrimagnetic material $Ba_3Co_2Fe_{24}O_{41}$, pre-aligned in a magnetic field and sintered at various temperatures, have been examined for preferred orientation. Schulz's reflexion technique and the standardizing method of Holland were used to determine quantitative pole figures of several lattice planes. The texture bears a close resemblance to a 'fan texture' in which the crystallites have their basal planes parallel to a preferred direction. The sharpness of the texture increases with increasing sintering temperature. At 1320 °C an exaggerated grain growth takes place. Inhomogeneity of the magnetic field throughout the sample results in local differences in orientation.

Introduction

The compound $Ba_3Co_2Fe_{24}O_{41}$ (Co_2Z) belongs to the ferroxplana, a group of magnetic materials having a hexagonal crystal structure (Braun, 1957). As a result of ferrimagnetism, Co_2Z exhibits magnetic anisotropy: above 480 °K the c axis is a preferred direction for magnetization; between 220 °K and 480 °K the basal plane is a preferred plane and below 220 °K the preferred directions form a cone (Smit & Wijn, 1959).

A powder of Co_2Z was pressed in a magnetic field at room temperature. Consequently the unicrystalline particles were forced to align themselves so that their planes of preferred magnetization were parallel to the direction of the magnetic field. In this way the compact assumed what will be called a fan texture, which was preserved upon subsequent sintering.

A texture goniometer, operating on Schulz's reflexion method (Schulz, 1949), was used to determine the preferred orientation of the crystallites at the surface of the sample.

The degree of orientation was studied as a function of the sintering temperature, the position in the compact and the height of the compact from which the sample was taken.

Model of the ideal fan texture

According to Stuyts & Wijn (1957), the crystallites in an ideally oriented sample of a hexagonal ferrimagnetic material, in which the basal plane is the plane of easiest magnetization, are arranged in the following way (Fig. 1):

(1) their basal planes are parallel to the field direction;

(2) their c axes are distributed at random in a plane perpendicular to the field direction;

(3) the direction of the remaining crystallographic axes is arbitrary, so long as conditions (1) and (2) are fulfilled.

A representation of this type of texture (fan texture), is given in Figs. 2, 3 and 4. The corresponding pole figures are obtained by choosing either the equatorial plane or a plane through $z\bar{z}$ as a plane of projection. The direction $z\bar{z}$ is parallel to the field used during the orientation of the sample.

The pole figures of the (0001) planes are given in Fig. 2(*a*) and (*b*). The (0001) planes are all parallel to $z\bar{z}$ and their normals distributed at random in the equatorial plane, as has been stated above. Consequently, the (0001) pole density on the sphere is zero, except on the circle in the xy plane, which in stereographic projection is the line AB.

The pole figures of the (11$\bar{2}$0) planes are given in Fig. 3(*a*) and (*b*). For a given crystallite with the (0001) normal perpendicular to $z\bar{z}$, the (11$\bar{2}$0) normals can have any direction in a plane perpendicular to the (0001) normal. The probability P that a (11$\bar{2}$0) pole happens to be on the arc Δl is:

$$P_{(11\bar{2}0)} = \Delta l / 2\pi R \,,$$

where R is the radius of the stereographic sphere. When the number of (0001) normals on the equatorial plane is k, the total number of (11$\bar{2}$0) poles on the curved surface of a spherical segment $PQRS$ will be

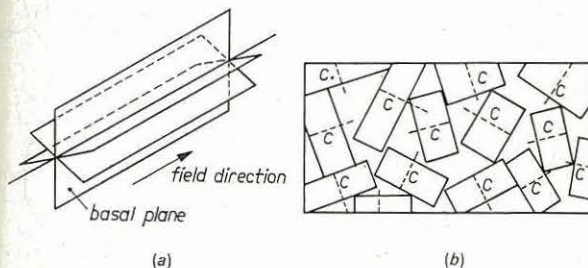$$N_{(11\bar{2}0)} = \frac{k \cdot \Delta l \cdot C}{2\pi R} \,,$$

Fig. 1. (*a*) Arrangement of the basal plane with respect to the field direction. (*b*) Orientation of the c axes of individual crystallites in a cross-section of the sample (field direction perpendicular to the paper).

where the constant C is the quotient of the multiplicity factors of the $(11\bar{2}0)$ and (0001) planes. The $(11\bar{2}0)$ pole density is given by the equation

$$D_{(11\bar{2}0)} = k \cdot \varDelta l \cdot C/2\pi R \cdot A,$$

where A is the area of the curved surface of a spherical segment $PQRS$ ($A = 2\pi R \cdot \varDelta l \cdot \sin\theta$). Substitution of the value of A yields

$$D_{(11\bar{2}0)} = k \cdot C/4\pi^2 R^2 \cdot \sin\theta.$$

We may conclude that $D_{(11\bar{2}0)}$ is proportional to $(\sin\theta)^{-1}$, θ being the polar angle shown in Fig. 3.

The pole figures of arbitrary $(hkil)$ planes are given in Fig. 4(a) and (b). The distribution of the $(hkil)$ poles on the sphere is somewhat more complicated. For a given crystallite with the (0001) normal perpendicular to $z\bar{z}$ the $(hkil)$ normal can have any direction on a conical surface. The cone is defined by its axis, which is the (0001) normal, and its apex angle ψ, which is the angle between the (0001) and $(hkil)$ normals of the same crystallite. The cone and reference sphere intersect along the circle $PQTSR$. The probability P that a given $(hkil)$ pole happens to be on the arc PQ of that circle is given by

$$P_{(hkil)} = \frac{\text{arc } PQ}{2\pi R \cdot \sin\psi}.$$

The total number of poles on the curved surface of the spherical segment $ABCD$ will be

$$N_{(hkil)} = \frac{k \cdot \text{arc } PQ \cdot C}{2\pi R \cdot \sin\psi}.$$

Again, the constant C is a quotient of multiplicity factors, in this case those of the $(hkil)$ and (0001) planes.

Since arc $PQ = \text{arc } EF \cdot \dfrac{\sin\theta \cdot \sin\psi}{(\sin^2\psi - \cos^2\theta)^{1/2}}$ (see Appendix),

the pole density is given by

$$D_{(hkil)} = \frac{N_{(hkil)}}{2\pi R \cdot \sin\theta \cdot \text{arc } EF}$$

$$= \frac{k \cdot C}{4\pi^2 R^2 (\sin^2\psi - \cos^2\theta)^{1/2}}.$$

For $90° + \psi \geq \theta \geq 90° - \psi$ the pole density is proportional to

$$(\sin^2\psi - \cos^2\theta)^{-1/2};$$

for $\theta < 90° - \psi$ $\Big\}$ the pole density is zero.
and $\theta > 90° + \psi$

It is to be noted that all the pole density distributions have axial symmetry with respect to the direction $z\bar{z}$ and inversion symmetry with respect to O.

In practice, deviation from the perfect orientation causes the poles to spread out from well-defined maxima into areas on the pole figure diagram, to an extent determined by the amount of deviation from the ideal orientation.

It might be expected that a [0001] fibre texture would be superimposed on the fan texture because the plate-like particles tend to align themselves with their basal planes perpendicular to the pressing direction (the plate surface is parallel to the basal plane).

Experimental

Preparation of the samples

Oriented specimens were prepared at Philips' Research Laboratories by filtering a slurry of Co_2Z powder (grain size approximately $1\mu m$) in acetone under pressure in the presence of an external magnetic field. This field could be applied either parallel with or perpendicular to the pressing direction. Particles able to rotate freely oriented themselves as described previously and were immobilized by compressing. The major part of the acetone was removed and the resulting cakes dried and then sintered in an oxygen
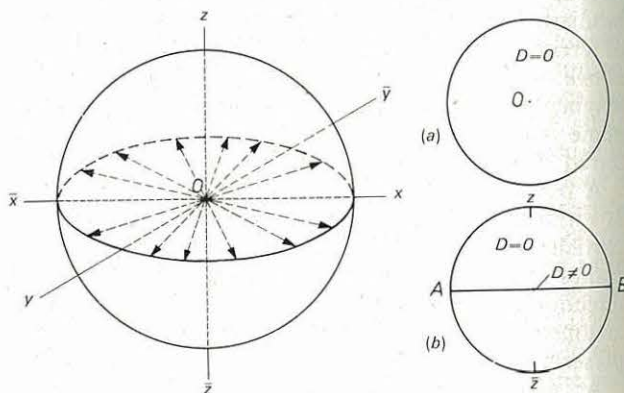
Fig. 2. Distribution of the (0001) normals. Pole figure (a) is the projection on the xy plane, (b) is the projection on a plane through $z\bar{z}$.
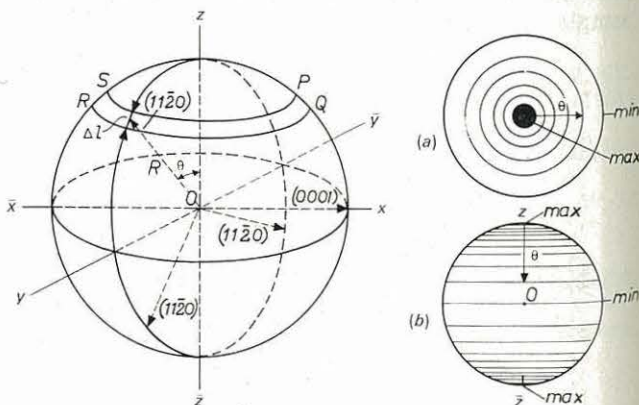
Fig. 3. Distribution of the $(11\bar{2}0)$ normals. The $(11\bar{2}0)$ normals of three crystals are shown in the Figure. Pole figure (a) is the projection on the xy plane, (b) is the projection on a plane through $z\bar{z}$.

atmospher
grain grow

Cylindri
diameter,
ways: para
compact
pressing d
was neces
sample su
cally. The
eter table
cylinder a
table.

Random
pressing t
tained in t
density eq

Measurem

The equ
was a type
on a modi
tion with
During the
eter table
normal to

Fig. 4. Dis

atmosphere at various temperatures in order to study grain growth and changes in texture.

Cylindrical samples, 7 mm in height and 15 mm in diameter, were drilled out of the filter compact in two ways: parallel (A, only the central portion of the filter compact was used) and perpendicular (B) to the pressing direction. In order to handle these samples it was necessary to embed them in 'Technovit'. The sample surfaces were ground and polished mechanically. The samples were firmly fixed to the goniometer table by means of screws, making sure that the cylinder axes were perpendicular to the mounting table.

Randomly oriented samples were prepared by compressing the powder isostatically. The compact obtained in this way was also sintered in order to get a density equal to that of the anisotropic samples.

Measurement technique

The equipment used to obtain the pole figure data was a type P.W. 1078 Philips texture goniometer based on a modified principle of Schulz (1949), in conjunction with the wide-range goniometer P.W. 1050. During the measurements the sample on the goniometer table was rotated over an angle α round an axis normal to its reflecting surface and simultaneously tilted over an angle φ round an axis lying in this surface. φ increased at a rate of $\frac{5}{8}$ degree.min^{-1} and α at a rate of 45 degree.min^{-1}, starting from $\alpha=\varphi=0$ at $t=0$. Simultaneously with these rotations, the sample oscillated back and forth in its reflecting plane over a distance of 5 mm.

An iron-target X-ray tube operated at 40 kV and 24 mA was used with a manganese filter. To reduce the influence of the remaining white radiation, the intensity of the diffracted beam was measured with a proportional counter fitted with a pulse-height discriminator. In this way spurious areas in the pole figures due to diffraction of white radiation were avoided. By using a 0·2 mm wide detector slit and Soller slits in the diffracted beam, adjacent reflexions such as 11$\bar{2}$0 and 0,0,0,18, with Bragg angles equal to 38·46 and 38·92° respectively, could be resolved.

Evaluation of measurements

A disadvantage of the reflexion method used is the change in focusing conditions with varying sample position, described by Chernock & Beck (1952). The defocusing of the diffracted beam was investigated by measuring the intensities of a strong reflexion from a non-oriented sample. A considerable loss in diffracted

Fig. 4. Distribution of the (hkil) normals. Pole figure (a) is the projection on the xy plane, (b) is the projection on a plane through zz̄.

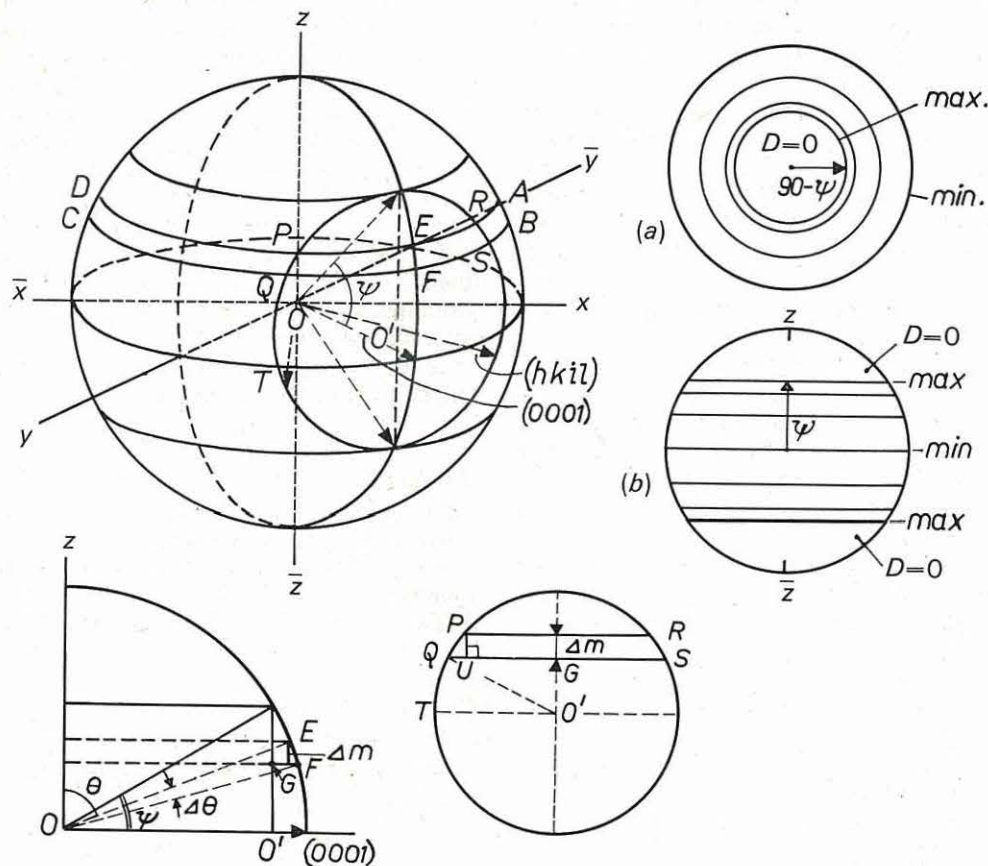intensity with increasing tilting angle φ was found even when the sample was accurately positioned in the goniometer. This gave rise to fallacious maxima in the centre of the pole figures. In order to eliminate the effect of defocusing, the intensity data were standardized according to a method of Holland (1964) after the usual correction for background:

$$I_{stand}(\varphi, \alpha) = \frac{I_{obs}(\varphi, \alpha) - I_{bg}(\varphi, \alpha)}{I_{n-or}(\varphi, \alpha) - I_{n-orbg}(\varphi, \alpha)}$$

$I_{stand}(\varphi, \alpha)$ = standardized intensity in position (φ, α)

$I_{obs}(\varphi, \alpha)$ = observed intensity of the oriented sample in that position

$I_{bg}(\varphi, \alpha)$ = average of the background intensities on both sides of the Bragg diffraction maximum of the oriented sample

$I_{n-or}(\varphi, \alpha)$ = observed intensity of the non-oriented sample

$I_{n-orbg}(\varphi, \alpha)$ = background intensity of the non-oriented sample

Pole figures were constructed by drawing iso-intensity contours for the reflexions listed in Table 1. By using the reflexion method, only regions up to 70° from the centre of the pole figures could be measured. In order to obtain a more complete description of the orientation, pole figures were constructed from two samples drilled out of the same filter cake; one parallel (out of the central portion) and one perpendicular to the pressing direction.

The change in texture with increasing sintering temperature was determined by measuring samples sintered at 1220, and 1280 or 1320 °C, from which the upper layer had been removed. By scanning the sample sintered at 1320 °C enormous fluctuations in the diffracted intensities were observed, which were due to coarse grains in the sample. In this case an equalizing curve had to be drawn before the standardized intensities could be calculated.

Transmission Laue photographs made with an X-ray microbeam of a 250 μm cross-section were used to determine the orientation of the individual crystallites in the coarse-grained material. The results of 30 Laue photographs of different regions in a thin slice (about 70 μm in thickness) of the sample which was sintered at 1320 °C, are as follows:

6 show Debye–Scherrer rings, caused by the reflexion from many small crystals;

4 show several superimposed Laue patterns;

20 show mainly one Laue pattern, from which the orientation of the axes of the crystal could be derived.

Results and discussion

The more important pole figures obtained in this investigation have been collected in Fig. 5, together with the pole figures of the ideal fan texture. The orientation of the samples with respect to field and pressing direction is also given in the Figure. Reasonable agreement with corresponding pole figures for an ideal fan texture leads to the conclusion that all samples possess this texture. Sintering at higher temperatures results in improved textural alignment, recognizable from the increase in maximum height in the pole figures. Compare, for example, the pole figures of sample no. 5 with those of no. 1 and the pole figures of sample no. 6 with those of no. 3. This increase must be ascribed to a growth of well-oriented crystallites at the expense of others.

Fig. 6 shows photomicrographs of the polished surface. By using polarized light the grain size after sintering at 1220, 1280 and 1320 °C could be determined. First, a normal crystal growth takes place, but at 1320 °C an exaggerated grain growth occurs. The sample sintered at that temperature shows large crystals of about 250 μm and many small crystals of about 10 μm, partly occuring as inclusions in the large ones.

The crystallographic orientations of 20 coarse grains of sample no. 5, determined by the Laue transmission X-ray technique, are plotted in the stereographic triangle shown in Fig. 7. The points represent the direction which is perpendicular to the sample surface (i.e. parallel with the field and pressing directions). A comparison is made of these data with the (0001) and (11$\bar{2}$0) pole figures from the same sample. In the (0001) pole figure of sample no. 5, shown in Fig. 5, the standarized intensity is zero for $\varphi < 70°$, which agrees with the results given in Fig. 7. The (11$\bar{2}$0) pole densities are derived from the results of the Laue photographs by using the equation

$$D_{(11\bar{2}0)} = N/A',$$

N = number of grains in interval $(\theta_1 - \theta_2)$, where θ is the angle between the [11$\bar{2}$0] direction and the normal to the sample surface,

A' = area of the curved surface of the spherical segment between θ_1 and θ_2.

In Table 2 the values of $D_{(11\bar{2}0)}$, derived from the Laue

Table 1. *Reflexions studied in this investigation*

Lattice plane	Intensity of the reflexion	Bragg angle (Fe $K\alpha$)	Angle ψ between the lattice plane and the (0001) plane
(000·14)	weak	30·08°	0°
(11$\bar{2}$0)	strong	38·46	90
(10$\bar{1}$·16)	strong	41·28	32° 45′
(11$\bar{2}$·10)	weak	44·43	60 38
(20$\bar{2}$·12)	weak	52·28	55 59

photographs of large crystals (column 2) are compared with the values of $D_{(11\bar{2}0)}$ derived from the pole figures based on all crystals (column 3). Although the data are somewhat scanty, they suggest that the texture of the large crystals is sharper than the texture of all crystallites in the sample. If we further assume that the twenty large crystals examined form a random sample of the entire population of coarse grains (>about
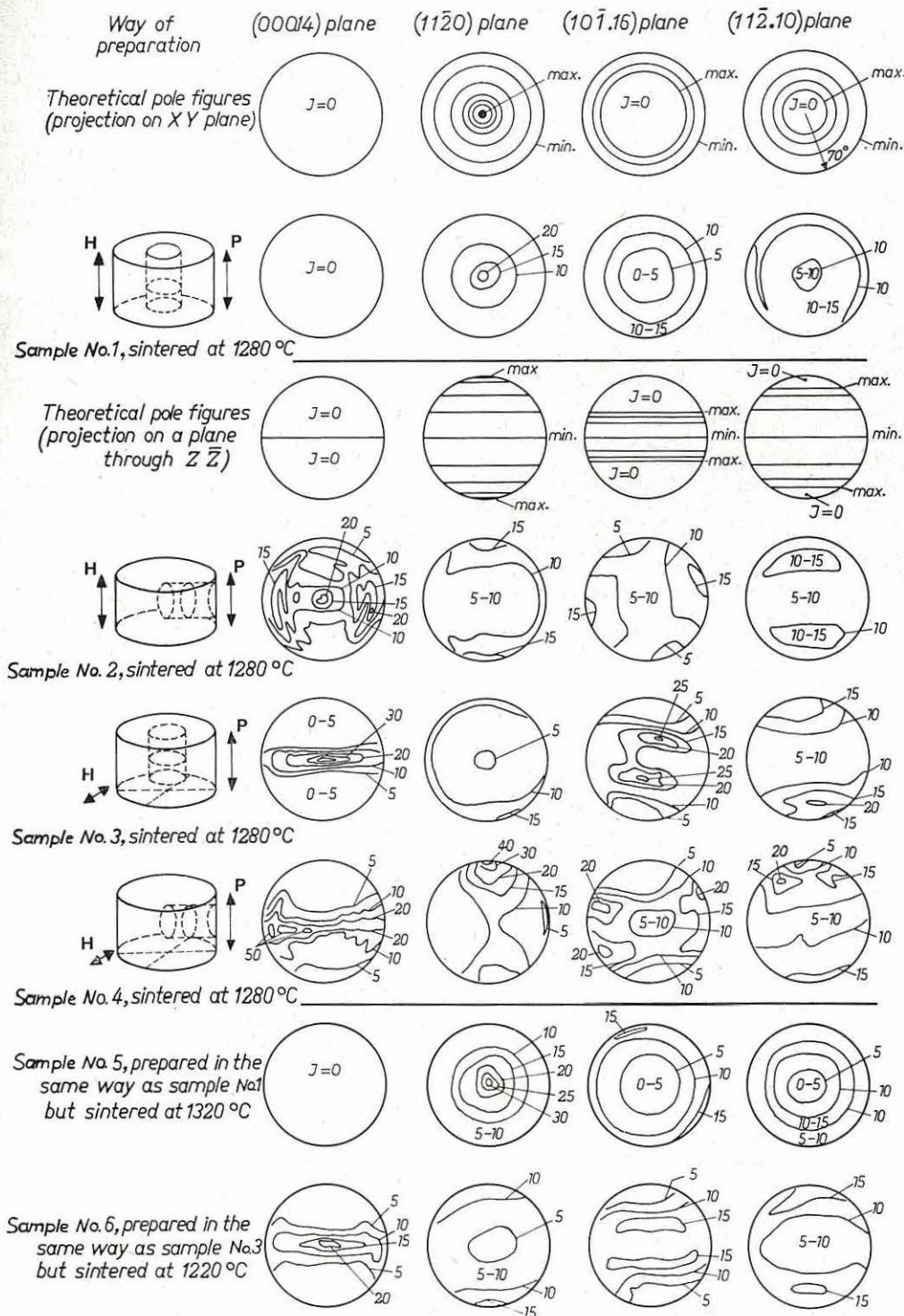

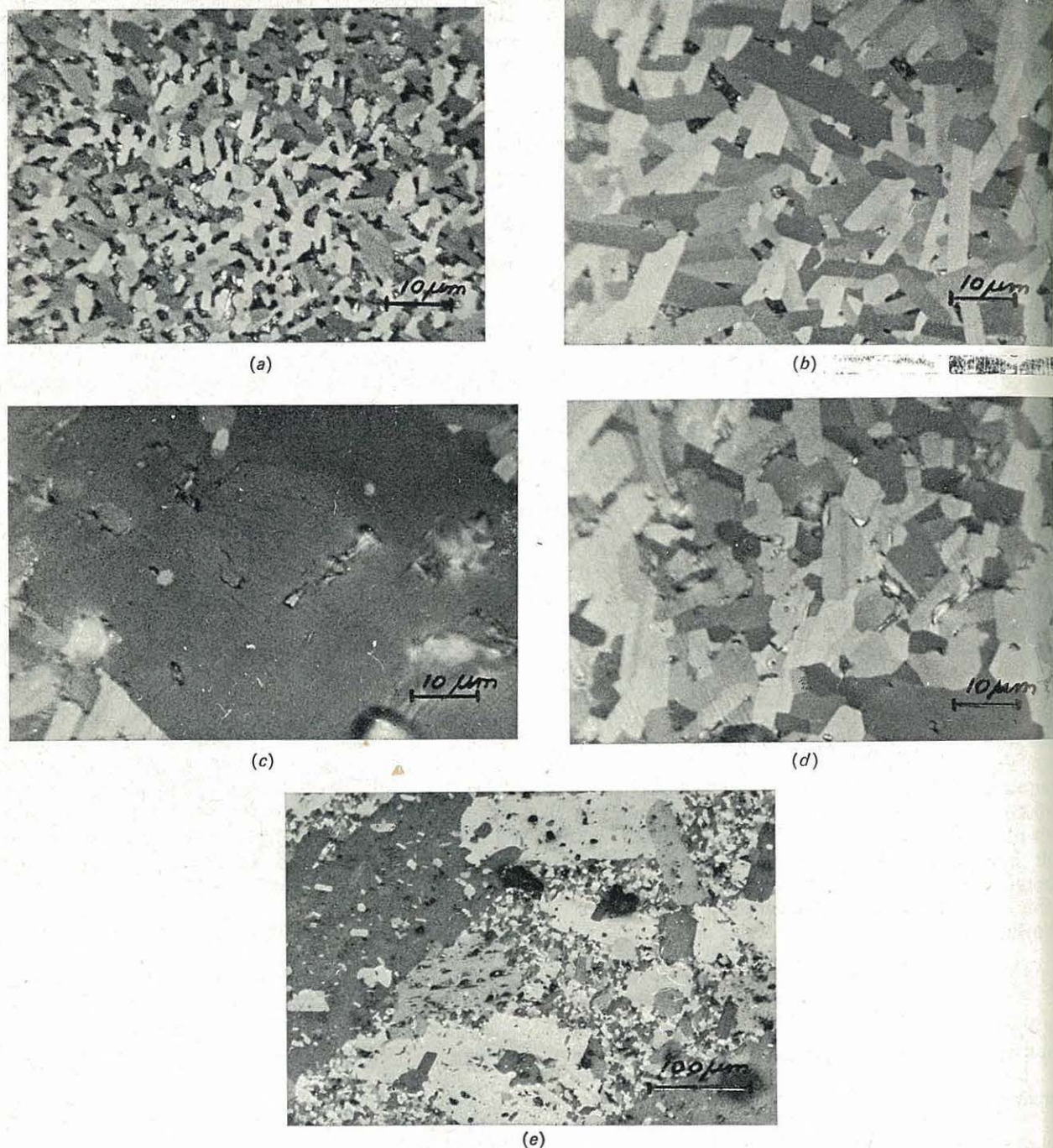Fig. 5. Theoretical and actual pole figures of several samples. H = field direction, P = pressing direction.

Fig. 6. Photomicrographs of several samples using polarized light. (a) Sample no. 7 prepared in the same way as sample no. 1, but sintered at 1220 °C. (b) Sample no. 1 sintered at 1280 °C. (c)–(e) Sample no. 5 prepared in the same way as sample no. 1, but sintered at 1320 °C; (c) large crystal, (d) small crystals, (e) large and small crystals.

150 μm), we are led to believe that the large grains are better oriented than the smaller ones.

We observed a sharpening of texture with increasing sintering temperature. It is natural to assume that this process results from the growth of well-oriented grains at the expense of less-well oriented crystallites. According to Stuyts (1956), the disappearance of less-well oriented crystals in a matrix of well-oriented crystals is very reasonable. In fact, this process has been observed by Stäblein & Willbrand (1966) and Stäblein
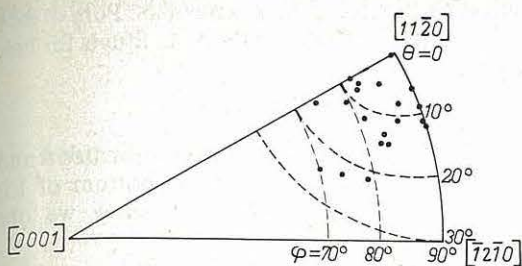
Fig. 7. Crystallographic orientations of 20 coarse grains in sample no. 5. θ and φ represent the angle between the [11$\bar{2}$0] or [1001] direction and the normal to the sample surface.

Table 2. *Pole densities $D_{(11\bar{2}0)}$ for various intervals of θ*

Column 2 was derived from the Laue photographs of large crystals. Column 3 was derived from the pole figures, based on all (large and small) crystals. Different arbitrary units are used in columns 2 and 3.

| $\theta_1-\theta_2$	$D_{(11\bar{2}0)} = N/A'$	$I_{stand} \propto D_{(11\bar{2}0)}$ (averaged over the interval $\theta_1-\theta_2$)
0–10	53	25
10–25	15	15

(1968) in barium-ferrite compacts with a [0001] fibre texture. Upon sintering the compacts at increasingly higher temperatures, this investigator observed a preferred grain growth with increasing sharpness of texture. Although our compacts had a fan texture, an analogous process of improvement in orientation through growth of well-oriented crystals seems quite obvious.

During filtration of a slurry of Co_2Z powder in acetone under one-sided pressure, and in the absence of an external magnetic field, a [0001] fibre texture appears in the residue as a result of the alignment of the plate-like particles. Such a texture was not present in our samples, as seen from the absence of a maximum in the centre of the (0001) pole figure of sample no. 1. This proves that the magnetic field exerts a stronger influence on the aligning process than does the pressing. No indication was found of a fibre texture which would have resulted from a particular preferred direction of magnetization in the basal plane.

Pole figures were also determined for areas on the probe surface [around B in Fig. 8(b) and around B_1 and B_2 in Fig. 8(a)] well outside the centre of the surface (A in the Figure). The maximum in each (11$\bar{2}$0) pole figure and the minimum in each (1,0,$\bar{1}$,16) pole figure
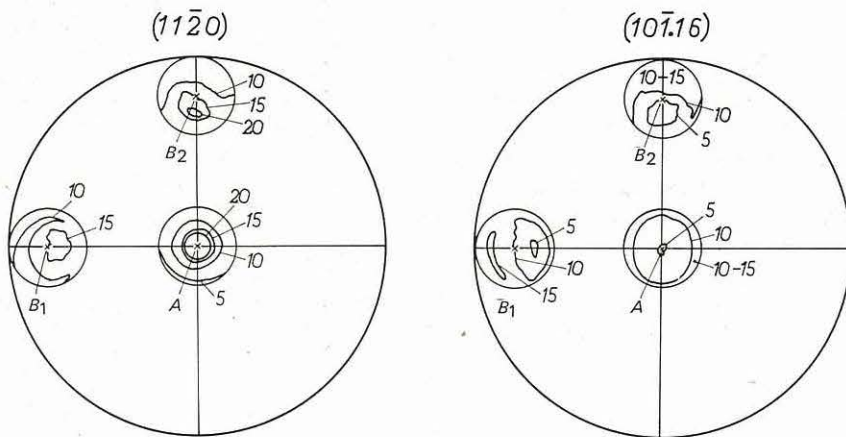
(a)
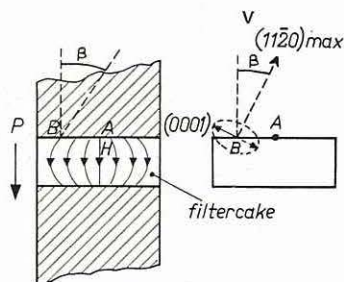
(b)

Fig. 8. (a) Interdependence of orientation and the region examined (A, B_1 and B_2) in the surface of the filter compact. The pole figures are shown in the sample surface for the sake of clarity. (b) Inhomogeneity of the field throughout the compact.

were shifted over about 30° towards the centre of the probe surface [Fig. 8(a)]. This is consistent with the inhomogeneous field-line pattern shown in Fig. 8(b). Since the (11$\bar{2}$0) pole density has its maximum along the field-line direction, the vector $V_{(11\bar{2}0\,max)}$, which is the direction of this maximum at point B, is inclined to the surface as shown in Fig. 8(b). This means that the maximum in the (11$\bar{2}$0) pole figure is shifted towards the probe surface centre A over an angle β indicated in the Figure.

Finally we have investigated whether or not a [0001] fibre texture accompanies the fan texture in samples taken from high filter cakes (the height of the filter cakes from which samples Nos. 1, 3, 5 and 6 were taken was about 9 mm). A coexistence of textures is conceivable for large filter-cake heights, since the magnetic field strength diminishes with increasing height, while the pressure inside the cake during pressing does not. For this purpose, pole figures were constructed for the area around A [Fig. 8(b)] in samples from filter cakes with a thickness varying from 5 to 25 mm. Hardly any difference was noticed between these pole figures, however. Important variations in pole density distributions along the cylinder axis of a 20 mm thick specimen proved also to be absent, as was verified by cutting successive slices from the sample normal to the cylinder axis.

Conclusions

When pressed in a magnetic field and sintered subsequently, the 'ferroxplana' compound develops a 'fan texture' which suppresses the [0001] fibre texture resulting from pressing of a powder of plate-shaped particles. The 'fan texture' sharpens if higher sintering temperatures are applied.

APPENDIX

In order to express arc PQ in the coordinates θ and ψ, we consider the two figures at the bottom of Fig. 4. From $GO' = R \cos \theta$ and $QO' = R \sin \psi$ we obtain

$$GQ = R (\sin^2 \psi - \cos^2 \theta)^{1/2}.$$

Since ΔPQU is similar to $\Delta QO'G$ we have

$$\frac{PQ}{PU} = \frac{QO'}{QG} = \frac{\sin \psi}{(\sin^2 \psi - \cos^2 \theta)^{1/2}}.$$

For infinitesimal values of $\Delta\theta$ we have

$$\text{arc } PQ = PQ, \quad PU = \Delta m = \text{arc } EF \times \sin \theta$$

and thus

$$\text{arc } PQ = \text{arc } EF \frac{\sin \theta . \sin \psi}{(\sin^2 \psi - \cos^2 \theta)^{1/2}}.$$

References

BRAUN P. B. (1957). *Philips Res. Rep.* **12**, 491.

CHERNOCK W. P. & BECK P. A. (1952). *J. Appl. Phys.* **23**, 341.

HOLLAND J. R. (1964). *Advanc. X-ray Anal.* **7**, 86.

SCHULZ L. G. (1949). *J. Appl. Phys.* **20**, 1030.

SMIT J. & WIJN H. P. J. (1959). *Ferrites*, p. 202. Eindhoven: Philips Technical Library.

STÄBLEIN H. & WILLBRAND J. (1966). *IEEE Trans. Magnetics*, **2**, 459.

STÄBLEIN H. (1968). *Tech. Mitt. Krupp Forschungs Berichte*, **26**, 81.

STUYTS A. L. (1956). *Chem. Weekblad*. **52**, 49.

STUYTS A. L. & WIJN H. P. J. (1957). *Philips Tech. Rev.* **19**, 209.